Nonlinear optical properties of low temperature annealed silicon-rich oxide and silicon-rich nitride materials for silicon photonics

S. Minissale,[1] S. Yerci,[2,a)] and L. Dal Negro[1,2,b)]
[1]*Photonics Center, Boston University, 8 Saint Mary's street, Boston, Massachusetts 02215-2421, USA and Division of Materials Science and Engineering, Boston University, 15 Saint Mary's Street, Brookline, Massachusetts 02446, USA*
[2]*Department of Electrical and Computer Engineering, Boston University, 8 Saint Mary's Street, Boston, Massachusetts 02215-2421, USA*

(Received 15 November 2011; accepted 17 December 2011; published online 10 January 2012)

We investigate the nonlinear optical properties of Si-rich silicon oxide (SRO) and Si-rich silicon nitride (SRN) samples as a function of silicon content, annealing temperature, and excitation wavelength. Using the Z-scan technique, we measure the non-linear refractive index n_2 and the nonlinear absorption coefficient β for a large number of samples fabricated by reactive co-sputtering. Moreover, we characterize the nonlinear optical parameters of SRN in the broad spectral region 1100-1500 nm and show the strongest nonlinearity at 1500 nm. These results demonstrate the potential of the SRN matrix for the engineering of compact devices with enhanced Kerr nonlinearities for silicon photonics applications. © *2012 American Institute of Physics*. [doi:10.1063/1.3675882]

Nonlinear silicon photonics has recently drawn significant attention due to the enhancement of numerous nonlinear optical processes that occur in silicon waveguides and resonator structures, enabling generation and processing of multiple optical signals within the widespread planar Si technology.[1–4] Recently, nonlinear silicon devices have been demonstrated for a wide range of applications such as sensing,[5,6] high rate signal processing,[3,4] broadband optical modulation,[7,8] classical and quantum metrology,[9,10] and broadband parametric frequency combs.[11,12] However, in bulk silicon, the nonlinear Kerr effect competes with parasitic nonlinear absorption effects (two-photon absorption, free carriers, defect-induced absorption) that are highly detrimental for the engineering of efficient nonlinear Si devices. As a result, there is presently a strong need to investigate third order optical nonlinearities in alternative Si-based materials platforms. Si-rich oxide (SRO) and silicon nitride materials have been proposed because of their enhanced properties with respect to bulk silicon,[13] and higher Kerr coefficient with reduced nonlinear absorption has been recently demonstrated. Moreover, Si-rich silicon nitride (SRN) has been intensively investigated for the engineering of light-emitting photonic crystal nanocavity devices and electroluminescent diodes,[14,15] but very little is known on the nonlinear optical properties of SRN compared to SRO materials.

In this paper, we perform a systematic study and a comparison between the third-order nonlinear optical properties of SRN and SRO samples fabricated by reactive magnetron sputtering as a function of the excess Si concentration and for low annealing temperatures below 700 °C, which guarantees full compatibility with complementary metal oxide semiconductor (CMOS) technology. Additionally, for the best SRN samples, we also investigate the dependence of their nonlinear optical properties on excitation wavelength.

SRN films with Si concentrations ranging between 52 and 70 at. %, as determined by energy-dispersive X-ray spectroscopy, and thicknesses of 350 nm were fabricated by N_2 reactive magnetron sputtering using Si target. The relative concentrations of Si and N atoms in the samples were controlled by varying the N_2/Ar gas flow ratio. Similarly, SRO samples were fabricated by O_2 reactive magnetron sputtering with the Si concentrations between 40 and 80 at. %, and the relative concentration of Si and O was adjusted by varying the O_2/Ar gas flow ratio during growth. Post growth annealing processes were performed for both set of samples using a rapid thermal annealing furnace at temperatures ranging between 200 and 700 °C for a fixed duration of 200 s. Z-scan nonlinear measurements were performed using a mode-locked Ti:sapphire laser (Mai Tai HP, Spectra Physics), with laser pulse duration of 100 fs and a repetition rate of 80 MHz, coupled to an electro-optical Pulse Peaker modulator (Conoptics 360-80) that varies the repetition rate of the pulses.

The pump beam was focused on the samples using a lens with 10 cm focal length and the beam waist, as measured by the knife-edge technique, was 100 μm at 800 nm. The pump wavelength was tuned using an optical parametric amplifier (Auto Inspire 100, Spectra Physics) coupled to the Ti:sapphire laser.

Examples of representative Z-scan traces measured in open and closed/open aperture configurations for SRN and SRO samples are shown in Fig. 1. By fitting Z-scan traces to an established theoretical model (Fig. 1), we can unambiguously extract the values of the nonlinear absorption coefficient β and the nonlinear refractive index n_2,[16] respectively (see Ref. 17 for a detailed description of the technique).

It is worth noticing that the Z-scan traces in open aperture show a peak in transmission in contrast to previous

a)Present address: Department of Mechanical Engineering, Massachusetts Institute of Technology, Cambridge, Massachusetts 02139, USA.
b)Author to whom correspondence should be addressed. Electronic mail: dalnegro@bu.edu.

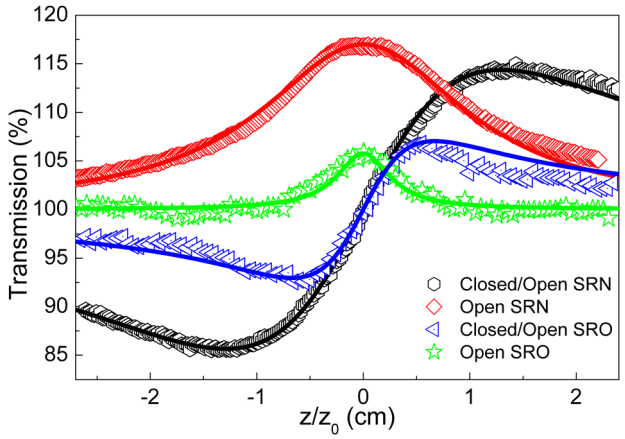

FIG. 1. (Color online) Typical Z-scan curves for SRN and SRO. Open aperture configuration (red diamonds and green stars, for SRN and SRO, respectively) and ratio of closed aperture to open aperture configuration (black hexagons and blue triangles, SRN and SRO, respectively). Continuous lines are fit to the standard theoretical model for Zscan.

reports on nanocrystal systems, where a transmission dip is observed instead. This discrepancy can be attributed to the different absorption mechanism characteristic of low temperature annealed samples, which is associated to the presence of localized bandtail states, in contrast to the behavior of nanocrystals samples annealed at higher temperatures.

In Figure 2, we show all the measured n_2 and β values collected for SRO and SRN samples as a function of the excess Si concentration (defined as the measured silicon concentration subtracted from the one at the equilibrium stoichiometry) and for different annealing temperatures. One can notice in Fig. 2 that both sets of samples display a clear superlinear dependence of the nonlinear parameters on the Si excess, as previously reported by Hernandez *et al*. for SRO samples.[18]

In the case of samples containing Si nanocrystals in a silicon oxide matrix,[18–20] the power law dependence of the nonlinearity with respect to the Si content has been previously interpreted as due to the role of quantum confinement on the third order susceptibility of single nanocrystals of varying sizes. Following this procedure, a $1/d^3$ dependence (with d the cluster diameter) on Si concentration has been derived. However, more recently the contribution of defects states to the nonlinear response of SRO samples annealed at lower temperatures (<800 °C) has also been discovered,[21] highlighting the complex interplay between optical nonlinearities, structural inhomogeneities, and defect centers in nonstoichiometric suboxides. Quantum confinement effects cannot explain the increase of optical nonlinearity with excess Si measured in our samples. In fact, annealing temperatures between 200 and 700 °C are not enough to nucleate Si nanocrystals in SRO and SRN matrices.[22] Therefore, the strong dependence of nonlinear coefficients on excess Si in our films could be attributed either to the nonlinear response of small amorphous nanoclusters formed at low temperatures[23,24] or to the density modulation of absorbing states in the band-tails of the amorphous matrices.[22] In order to distinguish between these two possible interpretations, we performed Z-scan measurements of n_2 and β as a function of the average excitation intensity. The results, shown in Fig. 3, demonstrate a linear dependence of the nonlinear coefficients on pump power, which is consistent with direct photon absorption from defect states or band-tail states for both SRO and SRN. This behavior contrasts with the expected quadratic dependence that characterizes the electronic nonlinearities of nanostructures (i.e., crystalline and amorphous), such as two photon absorption, in which a high energy transition is attained by the absorption of two low energy photons.

Once n_2 and β have been independently determined, a nonlinear figure of merit (NFOM) can be defined as $\beta\lambda/n_2$ to assess the strength of nonlinearity with respect to parasitic absorption processes. The NFOM is plotted in Fig. 4 for the two representative sets of samples as a function of the annealing temperature and for different values of excess Si. By definition, at a fixed wavelength, a small value of NFOM

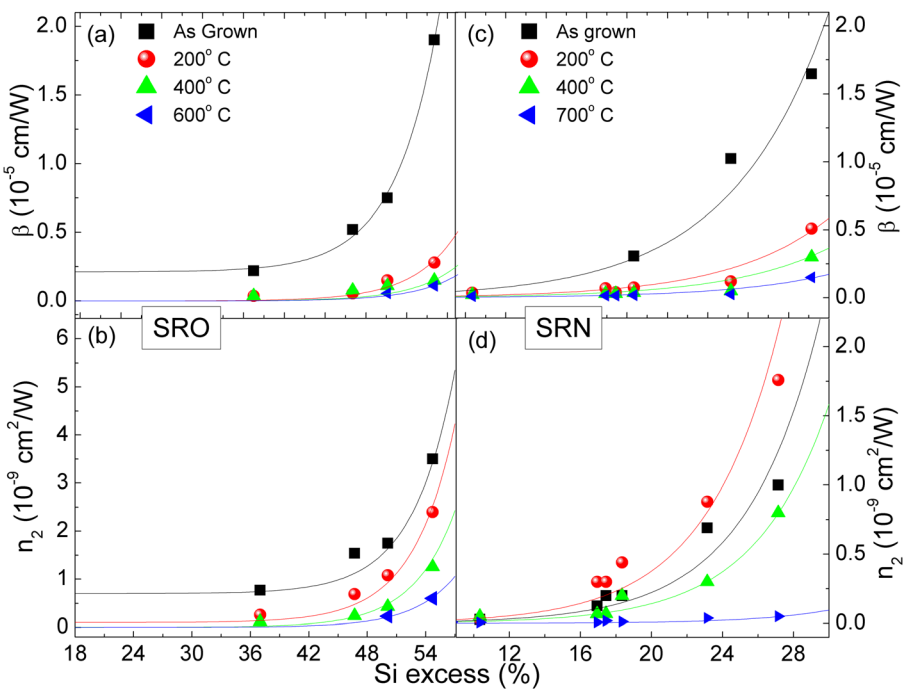

FIG. 2. (Color online) (a) and (b) show nonlinear absorption β and nonlinear refractive index n_2 as a function of Si excess for SRO, (c) and (d) for SRN. For both matrices, different annealing temperatures are reported. The superlinear dependence on Si excess is noticeable for all samples. Lines are guides to the eye.

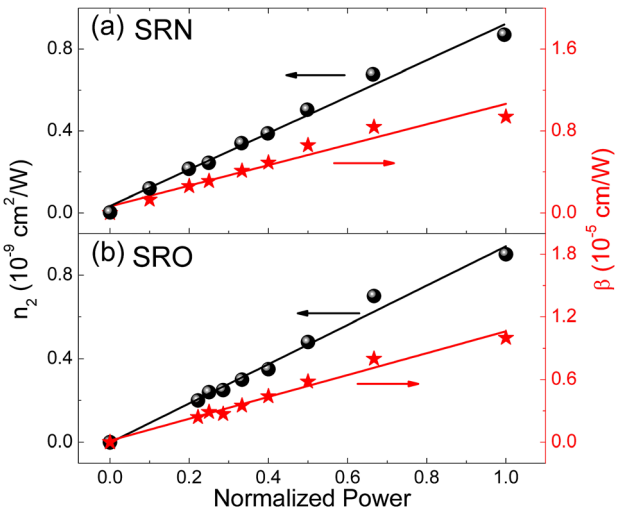

FIG. 3. (Color online) Nonlinear parameters n_2 and β in function of the normalized incident average power for SRN (a) and SRO (b).

(<1) is preferable, implying less contribution of the absorption with respect to the nonlinear refractive index n_2. In Fig. 4, panels (a) and (b) refer to SRN and SRO samples, respectively. In both cases, a non-monotonic behavior as a function of the annealing temperature can be noted for all samples regardless of different Si excess, similarly to what reported in Ref. 21 for silicon-rich oxide samples. In particular, we notice in Fig. 4 that in both sets of samples there is a region of optimal NFOM at low annealing temperatures (around 300 °C), where the β values, shown in Fig. 2, are the smallest regardless of the Si excess. We also demonstrated that the NFOM values for the SRO plotted in Fig. 4 are comparable to the ones reported in previous studies for Si nanocrystals annealed at much higher temperatures (>800 °C) in silicon oxide matrices.[18,21]

Finally, we characterized the wavelength dependence of the nonlinear refractive index and the nonlinear absorption of as-grown SRN sample. Our results are shown in Fig. 5, from which we see that n_2 and β behave very differently (i.e., they anti-correlate) as a function of wavelength. While the nonlinear refractive index n_2 increases from 800 nm to

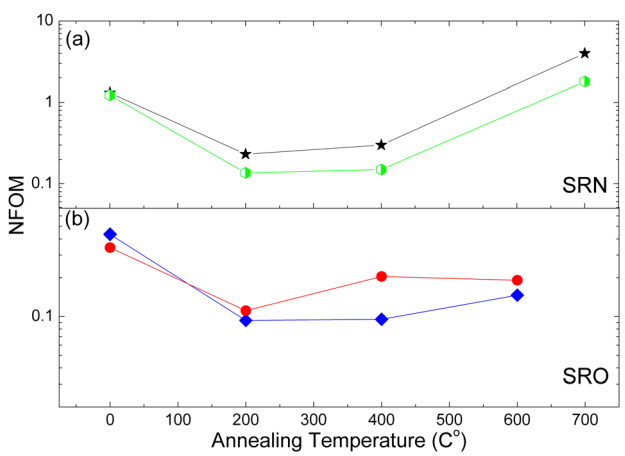

FIG. 4. (Color online) Nonlinear Figure of Merit $\beta\lambda/n_2$ as a function of the annealing temperature for different Si excess. Panel (a) shows the NFOM of SRN sample for Si excess for 27% (black stars), 18% (green hexagons). Panel (b) refers to SRO for 54% (blue diamonds) and 50% (red circles) Si excess, respectively.

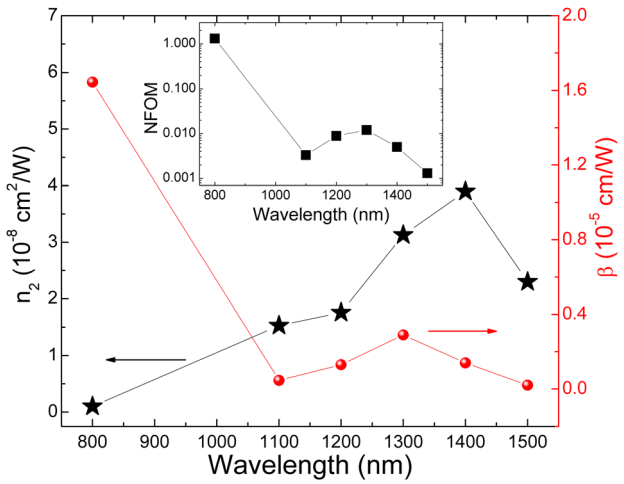

FIG. 5. (Color online) Nonlinear refractive index n_2 and absorption coefficient β as a function of the excitation wavelength for as-grown SRN with 27% Si excess. The inset displays the nonlinear figure of merit in the investigated wavelength range.

1500 nm, the nonlinear absorption follows an opposite trend, consistently with the decrease in band-tail absorption recently discovered at 1550 nm in SRN samples.[25] This peculiar behavior of the SRN band-tails is in contrast with what observed in samples containing Si nanocrystals embedded in silicon oxide,[26] where a square law dependence of free carrier losses versus wavelength was observed in the same spectral range. Differently, this study demonstrates that large refractive index nonlinearity can be obtained in amorphous SRN materials without nanocrystals due to the significant drop in band-tail absorption around 1500 nm. The lower absorption of the SRN material in the near-infrared spectral region compared to SRO has direct implications for the engineering of more efficient nonlinear optical devices since the measured NFOM for SRN at 1500 nm is almost one order of magnitude lower (i.e., better performances) than the one reported for SRO at the same wavelength.[18] In addition, due to the increased structural homogeneity of the amorphous SRN matrix, nonlinear waveguide and resonator structures can be fabricated with lower propagation losses,[2] enabling very efficient nonlinear silicon-based solutions for applications in the telecom wavelength range around 1500 nm.

In conclusion, we systematically measured the third order nonlinear optical properties of SRO and SRN samples as function of different fabrication parameters. Results demonstrate that the control of annealing temperature and Si excess are crucial in order to optimize the nonlinear performance of the materials and to minimize parasitic absorption losses in the 1500 nm spectral region. The nonlinear index values measured for low temperature annealed SRN materials in the infrared region 1100-1500 nm are the highest reported in a silicon-based material, making SRN an ideal candidate for device applications in the emerging field of nonlinear silicon photonics.

This work was partially supported by the AFOSR under MURI Award No. FA9550-06-1-0470, by the AFOSR DURIP program FA9550-10-1-0278, by the NSF Career Award ECCS-0846651, and by the AFOSR Award FA9550-10-1-0019.

[1]M. A. Foster, J. S. Levy, O. Kuzucu, K. Saha, M. Lipson, and A. L. Gaeta, Opt. Express **19**, 14233 (2011).
[2]J. S. Levy, A. Gondarenko, M. A. Foster, A. C. Turner-Foster, A. L. Gaeta, and M. Lipson, Nature Photon. **4**, 37 (2009).
[3]M. A. Foster, A. C. Turner, J. E. Sharping, B. S. Schmidt, M. Lipson, and A. L. Gaeta, Nature **441**, 960 (2006).
[4]V. R. Almeida, C. A. Barrios, R. R. Panepucci, and M. Lipson, Nature **43**, 1081 (2004).
[5]J. Leuthold, C. Koos, and W. Freude, Nature Photon. **4**, 535 (2010).
[6]A. M. Armani, R. P. Kulkarni, S. E. Fraser, R. C. Flagan, and K. J. Vahala, Science **317**, 783 (2007).
[7]J. T. Robinson, L. Chen, and M. Lipson, Opt. Express **16**, 4296 (2008).
[8]C. Koos, P. Vorreau, T. Vallaitis, P. Dumon, W. Bogaerts, R. Baets, B. Esembeson, I. Biaggio, T. Michinobu, F. Diederich *et al*., Nature Photon. **3**, 216 (2009).
[9]G. I. Stegeman and E. M. Wright, Opt. Quantum Electron. **22**, 95 (1990).
[10]P. Koonath, D. R. Solli, and B. Jalali, Appl. Phys. Lett. **91**, 061111 (2007).
[11]A. Thüring and R. Schnabel, Phys. Rev. A **84**, 033839 (2011).
[12]R. Schnabel, N. Mavalvala, D. E. McClelland, and P. K. Lam, Nat. Commun. **1**, 121 (2010).
[13]M. A. Foster, A. C. Turner, M. Lipson, and A. L. Gaeta, Opt. Express **16**, 1300 (2008).
[14]S. Yerci, R. Li, and L. Dal Negro, Appl. Phys. Lett. **97**, 081109 (2010).
[15]Y. Gong, M. Makarova, S. Yerci, R. Li, M. J. Stevens, B. Baek, S. W. Nam, R. H. Hadfield, S. N. Dorenbos, V. Zwiller *et al*., Opt. Express **18**, 13863 (2010).
[16]R. W. Boyd, *Nonlinear Optics* (Academic, Boston, 1992).
[17]M. Sheik-Bahae, D. Hutchings, D. J. Hagan, and E. W. Van Stryland, IEEE J. Quantum Electron. **27**, 1296 (1991).
[18]S. Hernández, P. Pellegrino, A. Martínez, Y. Lebour, B. Garrido, R. Spano, M. Cazzanelli, N. Daldosso, L. Pavesi, E. Jordana *et al*., J. Appl. Phys. **103**, 064309 (2008).
[19]J. M. Ballesteros, J. Solis, R. Serna, and C. N. Afonso, Appl. Phys. Lett. **74**, 2791 (1999).
[20]K. Imakita, M. Ito, M. Fujii, and S. Hayashi, J. Appl. Phys. **105**, 093531 (2009).
[21]M. Ito, K. Imakita, M. Fujii, and S. Hayashi, J. Appl. Phys. **108**, 063512 (2010).
[22]S. Yerci, R. Li, S. O. Kucheyev, T. van Buuren, S. N. Basu, and L. Dal Negro, Appl. Phys. Lett. **95**, 031107 (2009).
[23]F. Iacona, C. Bongiorno, C. Spinella, S. Boninelli, and F. Priolo, J. Appl. Phys. **95**, 3723 (2004).
[24]J. Warga, R. Li, S. Basu, and L. Dal Negro, Appl. Phys. Lett. **93**, 151116 (2008).
[25]R. Li, J. R. Schneck, J. Warga, L. D. Ziegler, and L. Dal Negro, Appl. Phys. Lett. **93**, 091119 (2008).
[26]R. D. Kekatpure and M. L. Brongersma, Opt. Lett. **34**, 3397 (2009).